

Spin current transmission in $Co_{1-x}Tb_x$ films

Li Wang(王力), Yangtao Su(苏仰涛), Yang Meng(孟洋), Haibin Shi(石海滨), Xinyu Cao(曹昕宇), and Hongwu Zhao(赵宏武)

Citation: Chin. Phys. B, 2022, 31 (**2**): 027504. DOI: 10.1088/1674-1056/ac3d83
Journal homepage: http://cpb.iphy.ac.cn; http://iopscience.iop.org/cpb

What follows is a list of articles you may be interested in

Perpendicular magnetic anisotropy of $Pd/Co_2MnSi/NiFe_2O_4/Pd$ multilayers on F-mica substrates

Qingwang Bai(白青旺), Bin Guo(郭斌), Qin Yin(尹钦), and Shuyun Wang(王书运)
Chin. Phys. B, 2022, 31 (**1**): 017501. DOI: 10.1088/1674-1056/ac20cc

Optimized growth of compensated ferrimagnetic insulator $Gd_3Fe_5O_{12}$ with a perpendicular magnetic anisotropy

Heng-An Zhou(周恒安), Li Cai(蔡立), Teng Xu(许腾), Yonggang Zhao(赵永刚), and Wanjun Jiang(江万军)
Chin. Phys. B, 2021, 30 (**9**): 097503. DOI: 10.1088/1674-1056/ac0db0

Magnetization and magnetic phase diagrams of a spin-1/2 ferrimagnetic diamond chain at low temperature

Tai-Min Cheng(成泰民), Mei-Lin Li(李美霖), Zhi-Rui Cheng(成智睿), Guo-Liang Yu(禹国梁), Shu-Sheng Sun(孙树生), Chong-Yuan Ge(葛崇员), and Xin-Xin Zhang(张新欣)
Chin. Phys. B, 2021, 30 (**5**): 057503. DOI: 10.1088/1674-1056/abd768

Field-induced N\'eel vector bi-reorientation of a ferrimagnetic insulator in the vicinity of compensation temperature

Peng Wang(王鹏), Hui Zhao(赵辉), Zhongzhi Luan(栾仲智), Siyu Xia(夏思宇), Tao Feng(丰韬), and Lifan Zhou(周礼繁)
Chin. Phys. B, 2021, 30 (**2**): 027501. DOI: 10.1088/1674-1056/abbbef

Computational study of inverse ferrite spinels

A EL Maazouzi, R Masrour, A Jabar, M Hamedoun
Chin. Phys. B, 2019, 28 (**5**): 057504. DOI: 10.1088/1674-1056/28/5/057504

RAPID COMMUNICATION

Spin current transmission in $Co_{1-x}Tb_x$ films

Li Wang(王力)[1,2], Yangtao Su(苏仰涛)[1,2], Yang Meng(孟洋)[1,2], Haibin Shi(石海滨)[1,2], Xinyu Cao(曹昕宇)[1,2], and Hongwu Zhao(赵宏武)[1,2,3,†]

[1] *Beijing National Laboratory for Condensed Matter Physics, Institute of Physics, Chinese Academy of Sciences, Beijing* 100190, *China*
[2] *School of Physical Sciences, University of Chinese Academy of Sciences, Beijing* 100049, *China*
[3] *Songshan Lake Materials Laboratory, Dongguan* 523808, *China*

(Received 2 October 2021; revised manuscript received 11 November 2021; accepted manuscript online 26 November 2021)

We investigate the spin to charge conversion phenomena in $Y_3Fe_5O_{12}$/Pt/$Co_{1-x}Tb_x$/Pt multilayers by both the spin pumping and spin Seebeck effects. We find that the spin transport efficiency is irrelevant to magnetization states of the perpendicular magnetized $Co_{1-x}Tb_x$ films, which can be attributed to the symmetry requirement of the inverse transverse spin Hall effect. Furthermore, the spin transmission efficiency is significantly affected by the film concentration, revealing the dominant role of extrinsic impurity scattering caused by Tb impurity. The present results provide further guidance for enhancing the spin transport efficiency and developing spintronic devices.

Keywords: spin to charge conversion, perpendicular magnetized ferrimagnetic alloy, inverse spin Hall effect

PACS: 71.20.Eh, 72.25.–b, 72.25.Hg, 75.50.Gg **DOI:** 10.1088/1674-1056/ac3d83

1. Introduction

In spintronics, the interconversion between spin current and charge current arising from spin–orbit coupling (SOC) has received considerable attention as an effective way to manipulate spins by electrical means.[1,2] In a typical ferromagnetic/nonmagnetic metal (FM/NM) bilayer structure, pure spin currents are generated commonly by the spin pumping effect (SPE) and the longitudinal spin Seebeck effect (SSE) in the FM layer, then injected into the adjacent NM layer and converted into charge currents by the inverse spin Hall effect (ISHE).[3,4] Due to their strong SOC, 5d heavy metals, such as Pt, W, Ta, have been demonstrated to reveal appreciable spin to charge (S-C) conversion efficiency.[5–9] Recently, experimental studies show that the FMs also exhibit significant S-C conversion efficiency which is generally dependent on the orientation of the FM magnetization.[10–16] For example, based on an analysis of the ISHE characteristics, Das and Cramer *et al.* claimed the remarkable difference between the occasions of FM magnetization parallel and perpendicular to the spin polarization in permalloy (Py) and $Co_{60}Fe_{20}B_{20}$ films, respectively.[13,14] Zhu *et al.* further demonstrated that the Py magnetization greatly affects the spin relaxation process and interfacial spin injection efficiency.[15] However, a recent report by Tian *et al.* showed that the ISHE in pure Co is independent of the Co magnetization direction.[16] Nevertheless, the dependence of ISHE upon magnetization state reported by different groups still seems to be controversial. Moreover, in FMs, the additional symmetry breaking due to the presence of FM magnetization leads to generation of extra spin currents with different spin polarizations from those observed in nonmagnetic materials.[17–21] Therein, a magnetization-related ISHE, referred to the inverse transverse spin Hall effect (ITSHE) where spin current flows perpendicularly into magnetic layer with its spin polarization perpendicular to the magnetization, was proposed theoretically.[17] Until recently, experimental demonstrations of the ITSHE associated with symmetry properties of magnetization distribution remain rare. Therefore, a complete understanding of spin current transport in ferromagnets remains largely ambiguous. Experimental studies on fabricating various magnetic ordering structures and probing the impact of their magnetization process on the spin transport efficiency can help to further advance the development of spintronic devices.

For rare earth–transition metal (RE-TM) ferrimagnetic alloys, such as CoTb and CoGd,[22,23] the magnetic moments are antiferromagnetically coupled and uncompensated, thus can be tailored by varying the composition ratio or temperature. In addition, due to the strong SOC of the rare-earth element, RE-TM alloys are expected to have relatively high S-C converting efficiency. Hence, RE-TM ferrimagnetic alloys are endued with more versatility as S-C converting material. In this work, we demonstrate experimentally that the ITSHE is irrelevant to the magnetization states in the perpendicular magnetized system, and investigate the effect of SOC on the spin transport efficiency of $Co_{1-x}Tb_x$ alloys. We fabricate a special $Y_3Fe_5O_{12}$ (YIG)/Pt/$Co_{1-x}Tb_x$/Pt multilayered structure, where the magnetization of the spin injecting YIG layer and that of spin detecting $Co_{1-x}Tb_x$ layer are perpendicular to each other, while the Pt interlayer actually suppresses the ex-

†Corresponding author. E-mail: hwzhao@iphy.ac.cn

© 2022 Chinese Physical Society and IOP Publishing Ltd

change coupling between YIG and $Co_{1-x}Tb_x$. We show that the ITSHE signal remains unchanged under different magnetization states of $Co_{1-x}Tb_x$, consistent with the theoretical expectation. By varying the $Co_{1-x}Tb_x$ composition, we further show that the spin–charge conversion is significantly changed, demonstrating that the extrinsic impurity scattering dominates the transport process due to Tb impurity.

2. Method

A schematic diagram of the sample structure and measurement configuration is shown in Fig. 1(a). The YIG films (120 nm) are deposited on single crystalline $Gd_3Ga_5O_{12}$ (GGG) (111) substrates using RF magnetron sputtering at room temperature, followed by annealing in air atmosphere at 800 °C for 4 hours.[24,25] To avoid divergence between the magnetic properties of YIG films, all YIG films used in this experiment are prepared under the same condition in one single batch. Then, a series of Pt (3 nm)/$Co_{1-x}Tb_x$ (10 nm)/Pt (5 nm) multilayers are grown subsequently on the YIG film. The $Co_{1-x}Tb_x$ layer is prepared by co-sputtering Co and Tb targets with adjustable power. During the multilayer deposition, a hard mask is utilized to fabricate strip structures (3 mm in length and 0.2 mm in width). Next, using both SPE and SSE, the pure spin currents can be efficiently generated in the YIG/Pt (3 nm) bilayer and detected in the adjacent $Co_{1-x}Tb_x$ layer by ISHE. For the SPE measurement, a microwave excitation is generated by a GSG coplanar waveguide, and a static magnetic field H is applied in the film plane with an angle θ_H with respect to the y axis. For the SSE measurement, a longitudinal temperature gradient ∇T_Z is established by illumination of a perpendicularly incident white laser beam,[26,27] and the dc magnetic field H is applied along the y axis. The magnetic properties of YIG/Pt/$Co_{1-x}Tb_x$/Pt films are characterized by magneto-optical Kerr effect (MOKE) measurements. All measurements are performed at room temperature.

3. Result and discussion

First, we demonstrate that the pure spin current can be efficiently generated in the YIG/Pt (3 nm) bilayer by both SPE and SSE. Figure 1(b) shows the typical spectra of spin pumping voltage V_{SP} as a function of magnetic field H at $\theta_H = 90°$ and 270° respectively. The line shape of V_{SP} is fully symmetric with respect to the ferromagnetic resonance position, and can be well fitted using Lorentzian functions. No obvious dispersive line shape is observed due to the absence of anisotropic magnetoresistance (AMR) in YIG.[28,29] Then, the thermovoltage V_T is directly obtained from the same YIG/Pt sample under laser illumination with power up to 290 mW. As depicted in Fig. 1(c), the V_T signal presents extremely narrow hysteresis, in consistent with the steep magnetization reversal of YIG and typical characteristics of ISHE.[3] These measurements clearly indicate that the spin current can be reliably generated in YIG by both SPE and SSE, injected into the adjacent Pt layer, and then efficiently detected by ISHE.

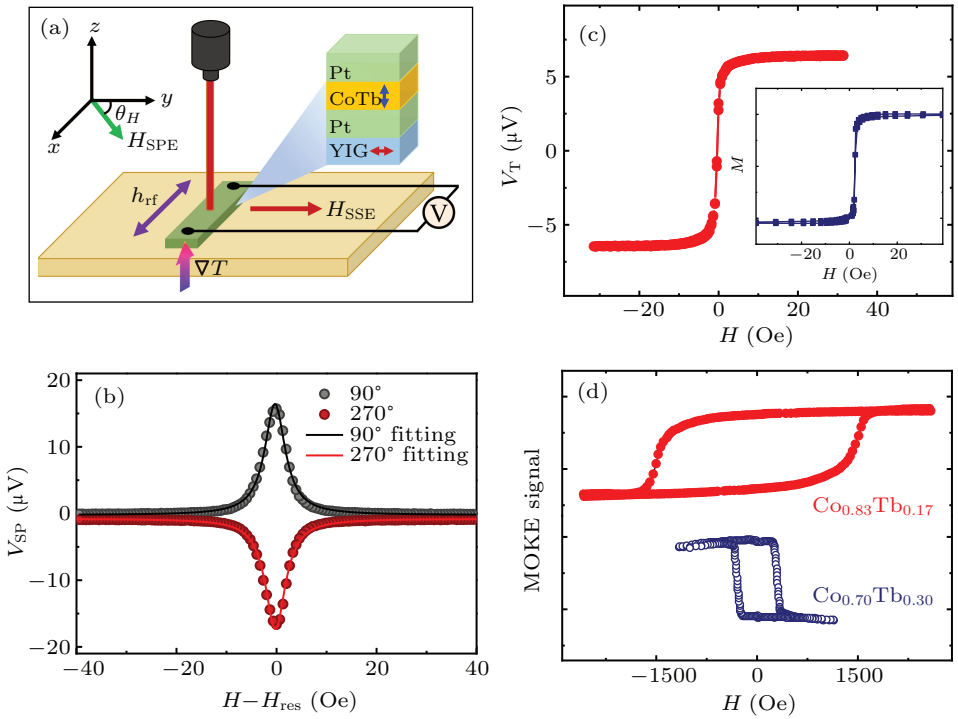


Fig. 1. (a) Schematic of the YIG/Pt/$Co_{1-x}Tb_x$/Pt structure and the measurement configuration. (b) V_{SP} versus H spectra of YIG/Pt (3 nm) with $P_{rf} = 80$ mW at 4 GHz. (c) Thermal voltage V_T as a function of H for YIG/Pt (3 nm) under white laser illumination of 290 mW. The inset shows the M–H loop of the YIG/Pt bilayer. (d) Representative MOKE hysteresis loops for YIG/Pt/$Co_{1-x}Tb_x$/Pt ($x = 0.17$, 0.30).

Next, we examine the magnetic properties of the YIG/Pt/$Co_{1-x}Tb_x$/Pt films. To avoid interference of the adjacent in-plane magnetized YIG layer, the MOKE measurements are performed under out-of-plane magnetic field to characterize the perpendicular magnetic anisotropy (PMA) of the $Co_{1-x}Tb_x$ films. Figure 1(d) displays typical hysteresis loops of $Co_{0.83}Tb_{0.17}$ and $Co_{0.70}Tb_{0.30}$, clearly demonstrating their strong PMA. It is noted that the polarity of the Kerr loop changes with Tb concentration, due to that the Kerr signal is primarily sensitive to the variation of Co sub-lattice around the magnetization compensation composition.[30,31]

Now we explore the spin transmission properties of the YIG/Pt/$Co_{1-x}Tb_x$/Pt structure by the SPE and SSE respectively. Figure 2(a) shows the field dependence of the spin pumping voltage V_{SP} of YIG/Pt/$Co_{0.70}Tb_{0.30}$/Pt under 4 GHz microwave excitation of 80 mW. Note that the V_{SP} exhibits a $\sin^3\theta$ dependence (Fig. 2(b)), which is a typical characteristic of the ISHE as a result of the in-plane rf field.[29,32] These results definitely confirm that the spin currents, generated in YIG/Pt by SPE, can propagate through $Co_{0.70}Tb_{0.30}$/Pt and indeed be detected by the ISHE. In addition, as shown in the inset of Fig. 2(b), both the linear dependence of V_{SP} on the rf power P_{rf},[5] and the dispersion relationship between the frequency f and the resonance field H_{res} which can be well fitted by the Kittle equation,[33] reconfirm the effectiveness of the Co–Tb detection layer. In contrast, the V_{SP} signal of the control sample of Si/Pt/$Co_{0.70}Tb_{0.30}$/Pt is totally invisible under the same measurement geometry, eliminating the possibility that the observed V_{SP} of YIG/Pt/$Co_{0.70}Tb_{0.30}$/Pt originates from the CoTb layer itself. For the SSE experiment, the thermal voltage V_T for YIG/Pt/$Co_{0.70}Tb_{0.30}$/Pt is measured with the magnetic field applied in the film plane under a laser power of 290 mW. Figure 2(c) shows the magnetic field dependence of V_T of YIG/Pt/$Co_{0.70}Tb_{0.30}$/Pt, and the magnitude of V_T is proportional to the illuminating laser power P_{Laser} (see Fig. 2(d)), in well agreement with the SSE features in the longitudinal configuration.[3,36] Similarly, the absence of V_T of the control sample Si/Pt/$Co_{0.70}Tb_{0.30}$/Pt indicates that the spin current solely comes from YIG rather than $Co_{0.70}Tb_{0.30}$ layer (see Fig. 2(c)). Hence, both the SPE and SSE measurements clearly demonstrate that the spin current generated in YIG/Pt can be efficiently injected to the adjacent $Co_{0.70}Tb_{0.30}$ layer and detected through ISHE.

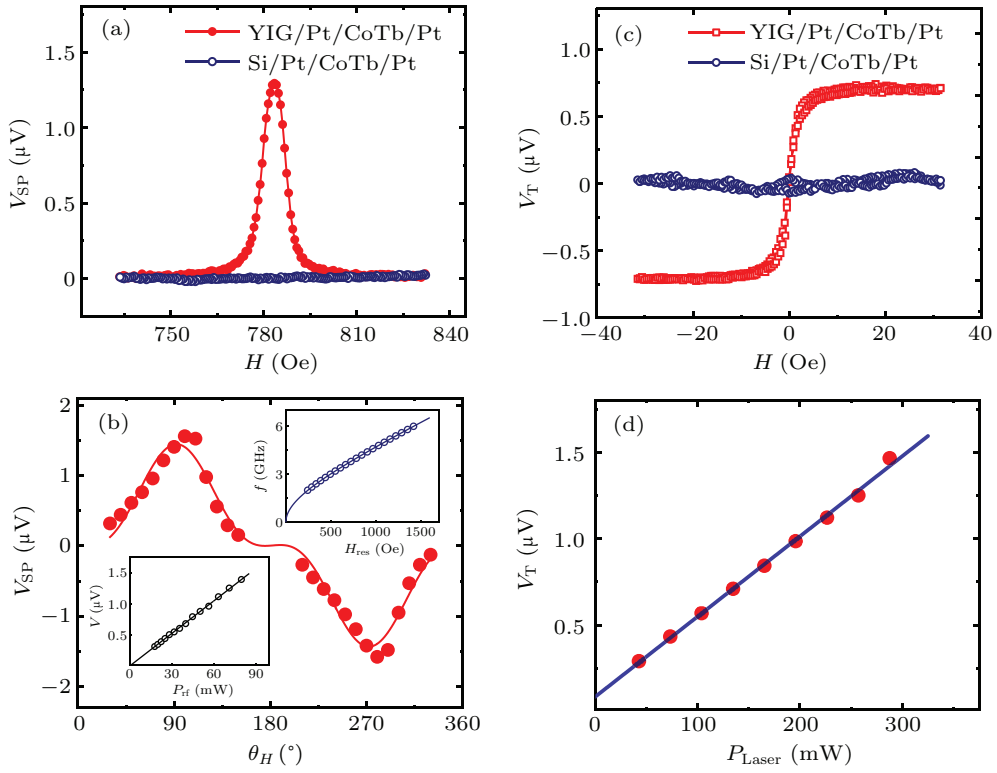


Fig. 2. (a) The V_{SP} versus H of YIG/Pt/$Co_{0.70}Tb_{0.30}$/Pt and Si/Pt/$Co_{0.70}Tb_{0.30}$/Pt structures at $\theta_H = 90°$. (b) Angular dependence of V_{SP}, the red curve is the best fit to V_{SP}. The insets show the microwave power dependence of V_{SP} and the H_{res} dependence of frequency f. (c) Field dependence of thermal voltage V_T in YIG/Pt/$Co_{0.70}Tb_{0.30}$/Pt and Si/Pt/$Co_{0.70}Tb_{0.30}$/Pt samples. (d) Laser power dependence of V_T.

To evaluate the impact of magnetic structure on spin-charge conversion, we examine the spin current transport properties of YIG/Pt/$Co_{0.70}Tb_{0.30}$/Pt with the Co–Tb layer set to different magnetization states. By applying DC (±4000 Oe) and AC fields normal to the film plane, the $Co_{0.70}Tb_{0.30}$ film is switched to saturated and demagnetized states, where $M_{CoTb} = M_s$, $M_{CoTb} = -M_s$ and $M_{CoTb} = 0$, respectively. As depicted in Fig. 3, there are no discernible differences in either V_T and V_{SP} signals obtained between different magnetized states. Note that the weak in-plane field used to magnetize YIG in both

SPE and SSE measurements will not alter the magnetization states of $Co_{0.70}Tb_{0.30}$ due to its strong PMA. Therefore, the magnetic structure of the $Co_{0.70}Tb_{0.30}$ layer hardly affects the S-C conversion efficiency in our experiment. In addition, the similar results have been obtained in other Co–Tb films with different composition (data not shown). According to Davidson's perspectives,[17] when spin currents flow along z axis into magnetic layer $\boldsymbol{m}$ where spin polarization $\boldsymbol{\sigma}\perp\boldsymbol{m}$, a magnetically related voltage signal would arise due to the ITSHE, satisfying the relation $V_{\mathrm{ITSHE}} \propto [\boldsymbol{m}\times(\boldsymbol{\sigma}\times\boldsymbol{m})]\times\hat{\boldsymbol{z}}$. It is easily seen that V_{ITSHE} should remain the same while $\boldsymbol{m}$ reverses its direction. For in-plane magnetized films, the direct experimental evidence has been reported in several YIG-based ferromagnetic heterostructures,[13,14,16] in good agreement with the theoretical prediction. For perpendicularly magnetized structure, such as CoTb in the present experiment, V_{ITSHE} is an even function of $\boldsymbol{m}_{\mathrm{CoTb}}$. Thus, the V_{ITSHE} remains unchanged for $M_{\mathrm{CoTb}} = M_{\mathrm{s}}$ and $M_{\mathrm{CoTb}} = -M_{\mathrm{s}}$.[20] On the other hand, in the perpendicularly demagnetized state, the CoTb layer consists of multi-domains with each domain magnetized randomly along z direction, $M_{\mathrm{CoTb}} = 0$, hence the sum of contributions to V_{ITSHE} from each domain should make no difference with the V_{ITSHE} whether $M_{\mathrm{CoTb}} = M_{\mathrm{s}}$ or $M_{\mathrm{CoTb}} = -M_{\mathrm{s}}$. Therefore, our measurements clearly reveal that the spin transport efficiency is independent of magnetization states of the perpendicular magnetized $Co_{1-x}Tb_x$ films, which is consistent with the theoretical model of ITSHE.

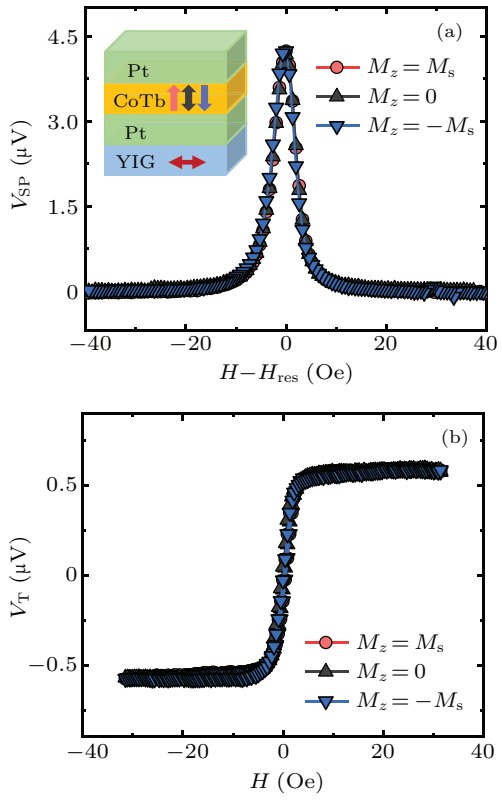


Fig. 3. (a) Field dependences of V_{SP} and (b) V_{T} of YIG/Pt/$Co_{0.70}Tb_{0.30}$/Pt at different magnetization states.

Next, we perform both SPE and SSE measurements on YIG/Pt/$Co_{1-x}Tb_x$/Pt structures with various Tb concentrations so as to investigate its impact on the spin transmission efficiency. To exclude the impact of the total resistance (R) of the sample on V_{ISHE}, the SPE and SSE signals have been normalized by R and plotted as a function of Tb composition, as shown in Fig. 4. It is clearly seen that both V_{SP}^R and V_{T}^R in the high Tb concentration region outweigh those in low Tb region, obviously indicating that the S-C conversion efficiency is significantly affected by the Tb impurity, and the higher Tb concentration directly leads to large spin–charge conversion efficiency. It is well accepted that the spin-dependent Hall effects (ISHE, SHE and AHE) share common microscopic origins: the intrinsic mechanism which is based on band structure of perfect crystals, and the impurity-related extrinsic mechanism including skew scattering and side-jump.[34,35] Due to the strong spin–orbit interaction of Tb, the extrinsic impurity scattering is expected to increase with increasing the Tb concentration, accordingly resulting in enhanced spin–charge conversion.[36–38] On the other hand, owing to the amorphous nature of the $Co_{1-x}Tb_x$ alloy films, the missing periodic order of crystal structure severely hampers the expressing of intrinsic contribution in the forms of crystal momentum.[39] Therefore, we cannot assess the intrinsic contribution of $Co_{1-x}Tb_x$ alloys in the present experiments, which needs to be explored in future study with optimized material design.

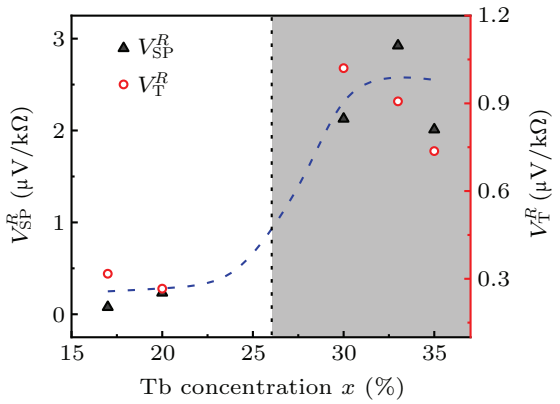


Fig. 4. Tb concentration dependences of normalized spin pumping voltage V_{SP}^R and thermal voltage V_{T}^R.

4. Conclusion

We experimentally study the spin transport efficiency of YIG/Pt/$Co_{1-x}Tb_x$/Pt structures. By the SPE and SEE measurements, we demonstrate experimentally that the ITSHE is irrelevant to the magnetization states in the perpendicular magnetized system. Moreover, the spin transport is significantly affected by varying the Tb concentration of the $Co_{1-x}Tb_x$ alloys, revealing the dominant role of extrinsic impurity scattering caused by Tb impurity.

Acknowledgements

Project supported by the National Key Basic Research Project of China (Grant No. 2016YFA0300600), the Strategic Priority Research Program of the Chinese Academy of Sciences (Grant No. XDB33020300), and the National Natural Science Foundation of China (Grant Nos. 11604375 and 11874416).

References

[1] Jungwirth T, Wunderlich J and Olejnik K 2012 *Nat. Mater.* **11** 382
[2] Hirohata A, Yamada K, Nakatani Y, Prejbeanu L, Diény B, Pirro P and Hillebrands B 2020 *J. Magn. Magn. Mater.* **509** 166711
[3] Uchida K, Xiao J, Adachi H, Ohe J, Takahashi S, Ieda J, Ota T, Kajiwara Y, Umezawa H, Kawai H, Bauer G E, Maekawa S and Saitoh E 2010 *Nat. Mater.* **9** 894
[4] Kajiwara Y, Harii K, Takahashi S, Ohe J, Uchida K, Mizuguchi M, Umezawa H, Kawai H, Ando K, Takanashi K, Maekawa S and Saitoh E 2010 *Nature* **464** 262
[5] Wang H L, Du C H, Pu Y, Adur R, Hammel P C and Yang F Y 2014 *Phys. Rev. Lett.* **112** 197201
[6] Hahn C, de Loubens G, Klein O, Viret M, Naletov V V and Ben Youssef J 2013 *Phys. Rev. B* **87** 174417
[7] Qu D, Huang S Y, Miao B F, Huang S X and Chien C L 2014 *Phys. Rev. B* **89** 140407
[8] Mosendz O, Pearson J E, Fradin F Y, Bauer G E, Bader S D and Hoffmann A 2010 *Phys. Rev. Lett.* **104** 046601
[9] Pai C F, Liu L, Li Y, Tseng H W, Ralph D C and Buhrman R A 2012 *Appl. Phys. Lett.* **101** 122404
[10] Miao B F, Huang S Y, Qu D and Chien C L 2013 *Phys. Rev. Lett.* **111** 066602
[11] Wang H, Du C, Chris Hammel P and Yang F 2014 *Appl. Phys. Lett.* **104** 202405
[12] Tsukahara A, Ando Y, Kitamura Y, Emoto H, Shikoh E, Delmo M P, Shinjo T and Shiraishi M 2014 *Phys. Rev. B* **89** 235317
[13] Das K S, Schoemaker W Y, van Wees B J and Vera-Marun I J 2017 *Phys. Rev. B* **96** 220408
[14] Cramer J, Ross A, Jaiswal S, Baldrati L, Lebrun R and Kläui M 2019 *Phys. Rev. B* **99** 104414
[15] Zhu Z Z, Zheng X L, Li G, Bai H, Su J, Zhang Y and Cai J W 2020 *Npg Asia Mater.* **12** 12
[16] Tian D, Li Y, Qu D, Huang S Y, Jin X and Chien C L 2016 *Phys. Rev. B* **94** 020403
[17] Davidson A, Amin V P, Aljuaid W S, Haney P M and Fan X 2020 *Phys. Lett. A* **384** 126228
[18] Humphries A M, Wang T, Edwards E R J, Allen S R, Shaw J M, Nembach H T, Xiao J Q, Silva T J and Fan X 2017 *Nat. Commun.* **8** 911
[19] Aljuaid W S, Allen S R, Davidson A and Fan X 2018 *Appl. Phys. Lett.* **113** 122401
[20] Yagmur A, Sumi S, Awano H and Tanabe K 2021 *Phys. Rev. B* **103** 214408
[21] Fan X, Mellnik A R, Wang W, Reynolds N, Wang T, Celik H, Lorenz V O, Ralph D C and Xiao J Q 2016 *Appl. Phys. Lett.* **109** 122406
[22] Ueda K, Mann M, Pai C F, Tan A J and Beach G S D 2016 *Appl. Phys. Lett.* **109** 232403
[23] Mishra R, Yu J, Qiu X, Motapothula M, Venkatesan T and Yang H 2017 *Phys. Rev. Lett.* **118** 167201
[24] Shi H B, Yan L Q, Su Y T, Wang L, Cao X Y, Bi L Z, Meng Y, Sun Y and Zhao H W 2020 *Chin. Phys. B* **29** 117302
[25] Yamamoto S, Kuniki H, Kurisu H, Matsuura M and Jang P 2004 *Phys. Stat. Sol. (a)* **201** 1810
[26] Weiler M, Althammer M, Czeschka F D, Huebl H, Wagner M S, Opel M, Imort I M, Reiss G, Thomas A, Gross R and Goennenwein S T B 2012 *Phys. Rev. Lett.* **108** 106602
[27] Agrawal M, Vasyuchka V I, Serga A A, Kirihara A, Pirro P, Langner T, Jungfleisch M B, Chumak A V, Papaioannou E T, and Hillebrands B 2014 *Phys. Rev. B* **89** 224414
[28] Mecking N, Gui Y S and Hu C M 2007 *Phys. Rev. B* **76** 224430
[29] Harder M, Cao Z X, Gui Y S, Fan X L and Hu C M 2011 *Phys. Rev. B* **84** 054423
[30] Alebrand S, Bierbrauer U, Hehn M, Gottwald M, Schmitt O, Steil D, Fullerton E E, Mangin S, Cinchetti M and Aeschlimann M 2014 *Phys. Rev. B* **89** 144404
[31] Takayama S, Niihara T, Kaneko K, Suglta Y and Ojima M 1987 *J. Appl. Phys.* **61** 7
[32] Harder M, Gui Y and Hu C M 2016 *Phys. Rep.* **661** 1
[33] Bhoi B, Venkataramani N, Aiyar R P R C, Prasad S, Kostylev M and Stamps R L 2013 *57th DAE Solid State Physics Symposium*, December 3–7, 2012, Bombay, India, p. 692
[34] Sinova J, Valenzuela S O, Wunderlich J, Back C H and Jungwirth T 2015 *Rev. Mod. Phys.* **87** 1213
[35] Onoda S, Sugimoto N and Nagaosa N 2006 *Phys. Rev. Lett.* **97** 126602
[36] Yagmur A, Sumi S, Awano H and Tanabe K 2020 *Phys. Rev. Appl.* **14** 064025
[37] Xu Z, Wong G D H, Tang J X, Liu E, Gan W L, Xu F and Lew W S 2020 *ACS Appl. Mater. Inter.* **12** 32898
[38] Ramaswamy R, Wang Y, Elyasi M, Motapothula M, Venkatesan T, Qiu X P and Yang H 2017 *Phys. Rev. Appl.* **8** 024034
[39] Xiao D, Chang M C and Niu Q 2010 *Rev. Mod. Phys.* **82** 1959